An Immune-Related lncRNA Model for Predicting Prognosis, Immune Landscape and Chemotherapeutic Response in Bladder Cancer

Jian Hou
The University of Hongkong-Shenzhen Hospital
Songwu Liang
The University of Hongkong-Shenzhen Hospital
Zhimin Xie
Zhuzhou Central Hospital
Genyi Qu (qugenyi@fjmu.edu.cn)
Zhuzhou Central Hospital
Yong Xu
Zhuzhou Central Hospital
Guang Yang
Zhuzhou Central Hospital
Cheng Tang
Zhuzhou Central Hospital

Research Article

Keywords: bladder cancer, immune-related lncRNA pairs, risk model, prognosis, immune infiltration, chemotherapeutic response

Posted Date: October 8th, 2021

DOI: https://doi.org/10.21203/rs.3.rs-953343/v1

Version of Record: A version of this preprint was published at Scientific Reports on February 25th, 2022.
See the published version at https://doi.org/10.1038/s41598-022-07334-w.

Abstract

Objective: Long noncoding RNAs (lncRNAs) participate in cancer immunity. Herein, we characterized the clinical significance of immune-related lncRNA model and its associations with immune infiltrations and chemosensitivity in bladder cancer.

Methods: Transcriptome data of bladder cancer specimens were employed from The Cancer Genome Atlas. Dysregulated immune-related lncRNAs were screened via Pearson correlation and differential expression analyses, followed by recognition of lncRNA pairs. Then, a LASSO regression model was constructed. Receiver operator characteristic curves of one-, three- and five-year survival were plotted. Akaike information criterion (AIC) value of one-year survival was determined as the cutoff of high- and low-risk subgroups. The differences in survival, clinical features, immune cell infiltrations and chemosensitivity were compared between subgroups.

Results: Totally, 90 immune-related lncRNA pairs were selected, 15 of which were put into the prognostic model. The area under the curves of one-, three- and five-year survival were 0.806, 0.825 and 0.828, confirming the favorable predictive performance of this model. According to the AIC value, we clustered subjects into high- and low-risk subgroups. High-risk score indicated unfavorable outcomes. This risk model was in relation to survival status, age, stage and TNM. In comparison to conventional clinicopathological characteristics, the risk model displayed higher predictive efficacy and was an independent predictor. Also, it could well characterize immune cell infiltration landscape and predict immune checkpoint expression and sensitivity to cisplatin and methotrexate.

Conclusion: This model conducted by paring immune-related lncRNAs regardless of expressions exhibited a favorable efficacy in predicting prognosis, immune landscape and chemotherapeutic response in bladder cancer.

Introduction

Bladder cancer is responsible for almost 170,000 deaths globally each year, mainly including two subtypes: non-muscle invasive (75%) and muscle invasive (25%) [1]. At present, cystoscopy represents the gold standard of clinical tools for diagnosing bladder cancer. Nevertheless, this procedure exhibits high invasiveness, and there is the consequence of false-negatives sporadically occurring due to the difficulty in detecting carcinoma in situ [2]. Despite much progress in therapeutic strategies like tumor resection, chemotherapy, and radiotherapy, survival duration and therapeutic responses vary among subjects. Due to high mutational burden, immune checkpoint inhibitors (ICIs) have been approved in advanced bladder cancer. However, the overall response rates are merely 15-25% [3], which highlights the importance of discovering biomarkers that may be predictive of treatment responses. As a highly heterogeneous malignancy, the etiology and clinicopathological manifestations vary among individuals. Growing evidence suggests that immunity is related to survival and therapeutic effects of bladder cancer [4]. For instance, targeting myeloid-derived suppressor cells (MDSCs) may heighten the therapeutic effects of ICIs

for cisplatin-resistant bladder cancer [5]. Tumor-infiltrating M2 macrophages are related to undesirable overall and disease-specific survival duration [6]. Hence, screening reliable immune-related prognostic indicators is of importance for bladder cancer.

Extensive RNA sequencing (RNA-seq) profiles by The Cancer Genome Atlas (TCGA) have suggested the implications of epigenetic, transcriptional, and post-transcriptional regulation of long noncoding RNAs (lncRNAs) in diagnosing and curing bladder cancer [7–9]. LncRNAs display higher specificity to biological states compared to coding RNAs [10]. Molecular characterizations have motivated to optimize actionable therapeutic strategies against bladder cancer [11]. As confirmed, lncRNAs mediate innate and adaptive immunity of bladder cancer through the functional states of immune cells and relevant pathways and genes [12]. For instance, lncRNA MIR4435-2HG contributes to unfavorable prognoses as well as high immune infiltrations in bladder cancer [13]. Recently, immune-related lncRNA signatures have been conducted for evaluating prognoses and immune infiltrations of bladder cancer [14–16]. Hence, this study attempted to develop a risk model constructed by immune-related lncRNA pairs for predicting the survival outcomes by modeling algorithms, paring, and iterations, immunotherapy, and chemotherapy of bladder cancer patients.

Results

Identifying dysregulated immune-related lncRNAs in bladder cancer

Here, transcriptome profiles of bladder cancer and normal specimens were obtained from TCGA and the lncRNAs were extracted. Immune-related lncRNAs that were distinctly correlated to immune-related genes were selected according to correlation coefficient>0.4 and p<0.001. As a result, 724 immune-related lncRNAs were identified (**Supplementary table 3**). Their expressions were compared between bladder cancer and normal specimens. Our data showed that 14 immune-related lncRNAs displayed down-regulation while 53 exhibited up-regulation in bladder cancer compared to normal specimens (Figure 1A, B and Table 1).

Table 1
A list of differentially expressed immune-related lncRNAs in bladder cancer.

LncRNAs	Control-mean	Tumor-mean	logFC	P-value	FDR
MAFG-DT	0.8136	3.2664	2.0053	5.72E-08	9.31E-07
ACTA2-AS1	3.8249	0.6005	-2.6711	1.69E-08	3.37E-07
AL353708.3	0.1422	0.6735	2.2437	1.94E-10	1.09E-08
FENDRR	14.6127	1.3817	-3.4027	1.15E-11	1.78E-09
AC112721.2	0.0316	0.6676	4.3990	2.30E-05	0.0001
AC006270.1	0.0965	0.8155	3.0798	6.13E-05	0.0003
AC113346.1	0.0252	0.8011	4.9891	1.91E-05	0.0001
AC005180.2	32.5163	1.3232	-4.6191	7.56E-11	5.85E-09
LINC00460	0.0044	0.8844	7.6590	3.78E-07	4.41E-06
AC093001.1	0.1245	5.9087	5.5686	0.0213	0.0356
AL359881.1	0.1413	0.7113	2.3321	0.0049	0.0100
AP003071.4	3.1926	0.5310	-2.5879	7.40E-11	5.85E-09
PICSAR	0.1230	4.2493	5.1110	0.0210	0.0352
AC134312.5	0.1421	0.6070	2.0945	0.0215	0.0358
AC026369.2	0.1270	0.7721	2.6033	4.99E-09	1.54E-07
AL591806.1	0.0736	0.5677	2.9480	2.63E-05	0.0001
AP001107.5	4.9308	0.3236	-3.9297	1.55E-12	4.80E-10
AC132807.2	0.2458	1.5154	2.6243	0.0035	0.0077
AC092171.4	0.2005	0.9546	2.2509	8.62E-09	2.03E-07
LINC01767	0.2183	0.8886	2.0252	0.0153	0.0270
AC112721.1	0.0080	0.5714	6.1660	2.27E-06	1.83E-05
AC010331.1	0.2417	1.0196	2.0768	2.10E-08	3.94E-07
AL591848.2	0.1662	0.8142	2.2927	0.0139	0.0247
LINC01082	18.0257	1.1959	-3.9138	8.85E-13	4.80E-10
LINC01705	0.1670	0.6708	2.0062	0.0002	0.0008
MYCL-AS1	0.1316	0.8034	2.6102	0.0003	0.0011

Abbreviations: logFC: log fold change; FDR: false discovery rate.

LncRNAs	Control-mean	Tumor-mean	logFC	P-value	FDR
ZNF710-AS1	4.9677	1.1662	-2.0907	1.18E-06	1.04E-05
AC099329.2	0.0516	0.9671	4.2290	0.0029	0.0067
LINC02577	0.0734	0.6493	3.1454	1.91E-05	0.0001
AL158166.1	0.1666	1.2025	2.8512	3.60E-07	4.29E-06
FIRRE	0.0665	1.0080	3.9228	2.01E-09	8.29E-08
MBNL1-AS1	8.0442	0.6428	-3.6456	5.72E-09	1.61E-07
AC100801.1	0.0128	0.9871	6.2697	0.0016	0.0042
LINC01615	0.2620	2.1924	3.0650	0.0011	0.0030
U62317.1	0.5744	3.9766	2.7914	3.10E-05	0.0001
AC129926.1	0.3629	2.1523	2.5684	0.0038	0.0082
LINC01614	0.2272	2.1317	3.2296	0.0018	0.0045
AL355916.1	0.1135	0.7073	2.6397	0.0004	0.0015
LINC02544	0.0978	0.9817	3.3274	0.0027	0.0063
AC099850.4	1.9189	9.1780	2.2579	2.45E-08	4.46E-07
AF127577.3	0.1440	1.2698	3.1409	0.0033	0.0073
LINC02820	0.4303	1.8480	2.1025	0.0003	0.0010
LINC02154	0.0166	2.6465	7.3188	4.56E-05	0.0002
SCAT1	0.0265	0.6981	4.7216	4.97E-07	5.49E-06
AC079466.1	0.0054	1.4797	8.0916	0.0089	0.0168
AL162424.1	7.0891	0.6299	-3.4923	1.84E-08	3.56E-07
AC053503.3	9.6868	1.0862	-3.1567	3.11E-11	3.85E-09
AC073365.1	0.1699	1.0171	2.5817	0.0246	0.0402
AC002401.4	0.5697	3.0533	2.4221	0.0163	0.0284
PGM5-AS1	59.866	2.0260	-4.8851	2.33E-12	4.80E-10
AC011503.2	0.2905	1.4524	2.3217	3.77E-08	6.67E-07
LINC02163	0.1588	0.9341	2.5560	3.52E-05	0.0002
AC007938.3	0.3067	1.2923	2.0748	9.59E-09	2.05E-07

Abbreviations: logFC: log fold change; FDR: false discovery rate.

LncRNAs	Control-mean	Tumor-mean	logFC	P-value	FDR
MIR100HG	7.4215	1.1565	-2.6819	4.04E-11	4.16E-09
AL161431.1	0.0659	5.4387	6.3660	2.47E-05	0.0001
AL161772.1	0.1690	0.8706	2.3647	6.80E-06	4.12E-05
AP000593.3	0.0881	0.6457	2.8737	0.0001	0.0004
AL513218.1	0.1969	0.8547	2.1181	2.94E-09	1.01E-07
LINC01711	0.0569	0.6419	3.4970	0.0003	0.0010
SCAT2	0.2505	1.3459	2.4256	1.49E-10	9.25E-09
NR4A1AS	5.9474	0.8542	-2.8000	9.30E-11	6.40E-09
AC007128.1	0.0996	0.6672	2.7438	2.05E-06	1.67E-05
AP005432.2	1.2159	16.1320	3.7300	0.0064	0.0125
LINC02195	0.3481	1.4088	2.0170	0.0039	0.0083
AC005180.1	23.4590	0.8483	-4.7895	7.88E-10	4.05E-08
TDRKH-AS1	0.13781	0.6742	2.2905	9.17E-09	2.03E-07
AC114488.1	0.3763	1.8766	2.3181	8.29E-05	0.0003
Abbreviations: logFC: log fold change; FDR: false discovery rate.					

Developing dysregulated immune-related lncRNA pairs and a risk model in bladder cancer

Utilizing an iteration loop and 0-or-1 matrices, 1871 dysregulated immune-related lncRNA pairs were recognized (**Supplementary table 4**). As depicted in univariate cox regression analyses, 90 lncRNA pairs could significantly impact bladder cancer subjects' survival (Table 2). Above pairs were screened through LASSO model. As a result, 15 dysregulated immune-related lncRNA pairs including MAFG-DT|SCAT2, ACTA2-AS1|LINC01705, LINC00460|PICSAR, AL359881.1|AC129926.1, LINC01767|AL161431.1, AC112721.1|LINC02154, AC010331.1|TDRKH-AS1, AL591848.2|AC100801.1, AL591848.2|AC005180.1, AL158166.1|AL355916.1, AC129926.1|SCAT2, AF127577.3|SCAT2, LINC02820|AC073365.1, AL161772.1|AP005432.2, and NR4A1AS|LINC02195 were put into this risk model (Figure 1C, D). Through uni- and multivariate cox regression analyses, these pairs displayed distinct associations with survival outcomes (Figure 1E, F). According to the coefficients and expressions of lncRNA pairs (Table 3), RS was calculated for bladder cancer subjects.

Table 2
Univariate cox regression analyses of immune-related lncRNA pairs that significantly affected bladder cancer prognoses.

LncRNA pairs	HR	HR.95L	HR.95H	P-value
MAFG-DT|AC011503.2	2.1709	1.4063	3.3513	0.0005
MAFG-DT|SCAT2	3.1762	1.9057	5.2937	9.25E-06
MAFG-DT|AC114488.1	1.8381	1.2055	2.8025	0.0047
ACTA2-AS1|LINC01767	1.7512	1.2655	2.4234	0.0007
ACTA2-AS1|LINC01705	0.6586	0.4796	0.9043	0.0098
AL353708.3|MIR100HG	0.6415	0.4651	0.8848	0.0068
FENDRR|LINC01767	1.7691	1.2468	2.5104	0.0014
AC112721.2|LINC01767	1.6876	1.2284	2.3184	0.0012
AC112721.2|LINC02195	1.6839	1.1687	2.4263	0.0052
AC112721.2|TDRKH-AS1	1.7458	1.2425	2.4530	0.0013
AC006270.1|MIR100HG	0.5957	0.4069	0.8720	0.0077
AC005180.2|AL591848.2	1.7067	1.2386	2.3517	0.0011
LINC00460|PICSAR	1.6665	1.1949	2.3241	0.0026
AL359881.1|AC129926.1	0.6330	0.4509	0.8887	0.0082
AP003071.4|LINC02195	1.6851	1.2270	2.3144	0.0013
PICSAR|AL161431.1	0.6513	0.4724	0.8979	0.0087
AC134312.5|LINC01767	1.5444	1.1127	2.1436	0.0094
AC134312.5|AC010331.1	1.5763	1.1346	2.1899	0.0067
AC134312.5|SCAT2	1.8170	1.2948	2.5497	0.0006
AC026369.2|AC010331.1	1.5782	1.1430	2.1791	0.0056
AC026369.2|MIR100HG	0.5911	0.4211	0.8297	0.0024
AC026369.2|SCAT2	1.7153	1.2011	2.4496	0.0030
AL591806.1|AL161431.1	0.6519	0.4720	0.9004	0.0094
AP001107.5|LINC01767	1.5468	1.1259	2.1249	0.0071
AC092171.4|AF127577.3	0.5907	0.4253	0.8204	0.0017

Abbreviations: HR: hazard ratio; HR.95L: 95% CI lower limit; HR.95H: 95% CI upper limit.

LncRNA pairs	HR	HR.95L	HR.95H	P-value
AC092171.4|MIR100HG	0.5595	0.4069	0.7693	0.0004
LINC01767|LINC01705	0.5810	0.4224	0.7989	0.0008
LINC01767|ZNF710-AS1	0.5396	0.3620	0.8044	0.0025
LINC01767|MBNL1-AS1	0.6130	0.4388	0.8563	0.0041
LINC01767|LINC01615	0.5847	0.4123	0.8292	0.0026
LINC01767|U62317.1	0.5831	0.3919	0.8675	0.0078
LINC01767|LINC01614	0.5849	0.4143	0.8256	0.0023
LINC01767|AL355916.1	0.5545	0.4036	0.7618	0.0003
LINC01767|LINC02544	0.5537	0.3983	0.7698	0.0004
LINC01767|MIR100HG	0.5820	0.4110	0.8242	0.0023
LINC01767|AL161431.1	0.6255	0.4552	0.8596	0.0038
LINC01767|AP000593.3	0.6184	0.4506	0.8486	0.0029
LINC01767|LINC01711	0.5652	0.4113	0.7768	0.0004
LINC01767|AC005180.1	0.6346	0.4621	0.8716	0.0050
AC112721.1|LINC02154	1.6769	1.2184	2.3079	0.0015
AC010331.1|LINC01705	0.6481	0.4675	0.8986	0.0093
AC010331.1|AL355916.1	0.5214	0.3667	0.7414	0.0003
AC010331.1|AF127577.3	0.5626	0.4042	0.7830	0.0007
AC010331.1|AC073365.1	0.6169	0.4342	0.8766	0.0070
AC010331.1|AC007938.3	0.6468	0.4643	0.9010	0.0100
AC010331.1|MIR100HG	0.6069	0.4422	0.8329	0.0020
AC010331.1|LINC01711	0.5298	0.3678	0.7632	0.0006
AC010331.1|NR4A1AS	0.5752	0.4179	0.7918	0.0010
AC010331.1|AC007128.1	0.5336	0.3867	0.7365	0.0001
AC010331.1|TDRKH-AS1	0.5747	0.4161	0.7938	0.0008
AL591848.2|LINC01705	0.6285	0.4578	0.8628	0.0041
AL591848.2|AC100801.1	0.6256	0.4484	0.8728	0.0058

Abbreviations: HR: hazard ratio; HR.95L: 95% CI lower limit; HR.95H: 95% CI upper limit.

LncRNA pairs	HR	HR.95L	HR.95H	P-value
AL591848.2|LINC01614	0.5812	0.4142	0.8156	0.0017
AL591848.2|LINC02544	0.6185	0.4495	0.8510	0.0032
AL591848.2|AC053503.3	0.5461	0.3976	0.7501	0.0002
AL591848.2|AL161431.1	0.6247	0.4547	0.8583	0.0037
AL591848.2|AC005180.1	0.4893	0.3559	0.6726	1.07E-05
LINC01082|LINC01705	0.6454	0.4697	0.8868	0.0069
LINC01082|MIR100HG	0.6509	0.4725	0.8967	0.0087
LINC01705|SCAT2	1.6358	1.1517	2.3232	0.0060
LINC01705|LINC02195	1.6179	1.1685	2.2400	0.0038
ZNF710-AS1|MIR100HG	0.6264	0.4565	0.8596	0.0038
ZNF710-AS1|AL513218.1	1.6645	1.1890	2.3301	0.0030
ZNF710-AS1|SCAT2	1.5430	1.1238	2.1186	0.0073
AL158166.1|AL355916.1	0.6091	0.4350	0.8530	0.0039
MBNL1-AS1|SCAT2	1.6495	1.1366	2.3938	0.0084
LINC01615|AL513218.1	1.6609	1.2072	2.2849	0.0018
LINC01615|SCAT2	1.5324	1.1146	2.1067	0.0086
LINC01615|LINC02195	1.8423	1.3186	2.5739	0.0003
AC129926.1|SCAT2	1.5904	1.1555	2.1889	0.0044
LINC01614|AC079466.1	1.9945	1.2464	3.1916	0.0040
LINC01614|SCAT2	1.5485	1.1282	2.1254	0.0068
LINC01614|AC007128.1	1.6830	1.2009	2.3584	0.0025
LINC01614|LINC02195	1.7120	1.2378	2.3679	0.0012
AL355916.1|AP005432.2	1.6000	1.1300	2.2655	0.0081
AL355916.1|TDRKH-AS1	1.6513	1.1741	2.3223	0.0040
LINC02544|AC011503.2	1.6707	1.1926	2.3403	0.0028
LINC02544|LINC02195	1.7000	1.2385	2.3335	0.0010
AF127577.3|AC007938.3	1.6687	1.1917	2.3367	0.0029

Abbreviations: HR: hazard ratio; HR.95L: 95% CI lower limit; HR.95H: 95% CI upper limit.

LncRNA pairs	HR	HR.95L	HR.95H	P-value
AF127577.3|AL513218.1	1.6737	1.2085	2.3179	0.0019
AF127577.3|SCAT2	1.9779	1.4063	2.7817	8.87E-05
LINC02820|AC073365.1	0.6539	0.4737	0.9023	0.0098
AC073365.1|AC114488.1	1.6172	1.1264	2.3217	0.0092
AC011503.2|MIR100HG	0.6088	0.4421	0.8383	0.0024
MIR100HG|SCAT2	1.7433	1.2622	2.4079	0.0007
MIR100HG|TDRKH-AS1	1.5835	1.1446	2.1905	0.0056
AL161431.1|LINC02195	1.5576	1.1348	2.1381	0.0061
AL161772.1|AP005432.2	1.6400	1.1777	2.2837	0.0034
AL513218.1|LINC01711	0.6116	0.4318	0.8662	0.0056
NR4A1AS|LINC02195	1.5426	1.1201	2.1245	0.0079
Abbreviations: HR: hazard ratio; HR.95L: 95% CI lower limit; HR.95H: 95% CI upper limit.				

Table 3
Regression coefficients of each factor in this prognostic immune-related lncRNA signature.

LncRNAs	Coefficient	HR	HR.95L	HR.95H	P-value
MAFG-DT|SCAT2	0.9052	2.4725	1.4417	4.2397	0.0010
ACTA2-AS1|LINC01705	-0.3363	0.7144	0.4986	1.0235	0.0668
LINC00460|PICSAR	0.3370	1.4007	0.9846	1.9928	0.0610
AL359881.1|AC129926.1	-0.6039	0.5467	0.3653	0.8179	0.0033
LINC01767|AL161431.1	-0.4304	0.6503	0.4532	0.9331	0.0195
AC112721.1|LINC02154	0.3135	1.3682	0.9684	1.9331	0.0754
AC010331.1|TDRKH-AS1	-0.5091	0.6010	0.4273	0.8454	0.0034
AL591848.2|AC100801.1	-0.3116	0.7323	0.4885	1.0977	0.1314
AL591848.2|AC005180.1	-0.7269	0.4834	0.3339	0.6999	0.0001
AL158166.1|AL355916.1	-0.5227	0.5929	0.4152	0.8468	0.0040
AC129926.1|SCAT2	0.5215	1.6846	1.1189	2.5364	0.0125
AF127577.3|SCAT2	0.8895	2.4339	1.6760	3.5346	2.97E-06
LINC02820|AC073365.1	-0.6777	0.5078	0.3566	0.7231	0.0002
AL161772.1|AP005432.2	0.4795	1.6153	1.1057	2.3599	0.0132
NR4A1AS|LINC02195	0.5227	1.6866	1.1873	2.3960	0.0035
Abbreviations: HR: hazard ratio; HR.95L: 95% CI lower limit; HR.95H: 95% CI upper limit.					

Evaluating the predictive performance of this risk model for prognoses

The cutoff value that differentiated bladder cancer subjects into high- and low-risk subgroups was 1.074 according to the AIC of one-year survival (Figure 2A). The AUC of one-year survival was 0.806 (Figure 2B). This indicated the favorable predictive efficacy of this risk model. Furthermore, we conducted the ROCs of three- and five-year survival. The AUCs of three- and five-year survival were 0.825 and 0.828, demonstrating that this risk model was also utilized for predicting three- and five-year clinical outcomes of bladder cancer (Figure 2C). According to the cutoff value, we clustered patients into high- and low-risk subgroups (Figure 2D). The distributions of survival status between subgroups were depicted in Figure 2E. High-risk subgroup possessed more dead patients in comparison to low-risk subgroup. The differences in survival duration were compared between subgroups. In Figure 2F, low-risk patients were predictive of favorable clinical outcomes compared to high-risk patients ($p<0.001$).

Associations between clinical features and this risk model

Figure 3A depicted the associations between clinical features and this risk model in bladder cancer. We found that the risk model was in relation to survival status ($p<0.001$), age ($p<0.05$), stage ($p<0.05$), T ($p<0.05$), N ($p<0.05$) and M ($p<0.05$) of bladder cancer patients. The differences in RS were compared among different subgroups of clinical features. As shown in our data, patients with dead status exhibited higher RS than those with alive status ($p<2.22e-16$; Figure 3B). In Figure 3C, patients in stage III-IV had elevated RS compared to those with stage I-II. Furthermore, >65 patients displayed increased RS than ≤65 subjects ($p=0.006$; Figure 3D). As depicted in Figure 3E, Subjects with T3-4 possessed higher RS than those with T1-2. Compared to patients with N0, increased RS was detected in those with N1-2 (Figure 3F). Also, higher RS was found in patients with M1 or Mx than M0 (Figure 3G). There were elevated RS in high grade than low grade specimens ($p=0.0045$; Figure 3H). Nevertheless, no significant difference in RS was found between female and male specimens (Figure 3I). Hence, this risk model might be relation to bladder cancer progression and metastases.

This risk model as an independent prognostic predictor

As depicted in univariate cox regression analyses, stage, T, N and risk model was in relation to bladder cancer prognoses (Figure 4A). This was indicative that above factors might impact patients' clinical outcomes. To evaluate the predictive independency, multivariate cox regression analyses were conducted. In Figure 4B, this risk model might be independently predictive of patients' prognoses. ROCs were conducted for comparing their differences in predictive performance of one-year survival. We found that this risk model possessed the highest AUC value (Figure 4C), demonstrating the favorable efficacy in predicting prognoses.

This risk model might predict immune cell landscape of bladder cancer

This study estimated immune cell infiltrations of bladder cancer specimens through XCELL, TIMER, QUANTISEQ, MCPCOUNTER, EPIC, CIBERSORT-ABS and CIBERSORT algorithms. Correlations between risk model and immune cell infiltrations were estimated via Spearson correlation test, as depicted in Figure 5. Our data demonstrated that high-risk specimens possessed increased infiltrations of myeloid dendritic cell, B cell native, macrophage M0 and M2, neutrophil and T cell CD8 (**Supplementary figure 1**).

Assessment of immune checkpoints with this risk model

Currently, ICIs have been approved for bladder cancer treatment. Hence, this study observed the correlations between this risk model and immune checkpoints in bladder cancer specimens. No significant differences in CTLA4 (Figure 6A), LAG3 (Figure 6B), PLD1 (Figure 6C), PD1 (Figure 6D) and TIGIT (Figure 6E) expressions were detected between high- and low-risk specimens. Nevertheless, GAL9 displayed elevated expression in low- than high-risk specimens (Figure 6F; $p<0.001$). Inversely, higher TIM-3 (Figure 6G; $p<0.05$) and PD1LG2 (Figure 6H; $p<0.001$) expressions were found in high-risk specimens in comparison to low-risk specimens.

Analysis of the associations between this risk model and chemosensitivity

The associations between this risk model and chemosensitivity were evaluated in bladder cancer specimens. Our data showed that high-risk patients exhibited decreased IC50 values of cisplatin in comparison to low-risk subjects (Figure 7A; p=0.043). This indicated that high-risk scores were predictive of higher sensitivity to cisplatin. In Figure 7B, reduced IC50 values of methotrexate were found in low-risk specimens than high-risk specimens (p=1.5e-08), demonstrating that low-risk scores were in relation to higher sensitivity to methotrexate. Furthermore, this study evaluated the differences in IC50 values of vinblastine (Figure 7C), gemcitabine (Figure 7D) and doxorubicin (Figure 7E) between high- and low-risk specimens. Nevertheless, no significant differences were found.

Discussion

LncRNAs have been confirmed to be in relation to cancer immunity regulation as well as tumor microenvironment in bladder cancer [17]. Several immune-related lncRNA models have been constructed in published literature [14,18,19]. Nevertheless, these signature models are developed on the basis of expression quantifications of immune-related lncRNAs. Herein, this study recognized the immune-related lncRNA pairs and constructed a reliable and independent risk model through combining two lncRNAs, not adopting their expression levels [20].

Here, we firstly screened immune-related lncRNAs by Pearson correlation analyses. Different from previous research, dysregulated immune-related lncRNAs were further identified by comparing their expressions between bladder cancer and normal specimens [14,21]. With cyclically single pairing methods with 0-or-1 matrices, we identified immune-related lncRNA pairs. Combining univariate analyses and LASSO model, we developed a risk model for bladder cancer. Not using the median RS as the cutoff value that differentiated bladder cancer subjects into high- and low-risk subgroups, the AIC value of one-year survival was determined as the optimal cut-off value [14,22,23]. Furthermore, this risk model possessed distinct associations with survival status, age, stage and TNM of bladder cancer. As depicted in multivariate regression analyses, RS might independently predict bladder cancer patients' OS. In comparison to other clinical features, RS displayed the highest AUC of one-year OS, indicating that this RS possessed the potential as a favorable predictor of bladder cancer. Moreover, this risk model was in relation to immune cell infiltrations and immune checkpoints. Intertumoral tumor-infiltrating immune cells may impact the responses to ICIs. Here, by comprehensively utilizing XCELL, TIMER, QUANTISEQ, MCPCOUNTER, EPIC, CIBERSORT-ABS and CIBERSORT algorithms, we characterized the correlations between risk model and immune cell infiltrations. High-risk specimens possessed elevated infiltration levels of myeloid dendritic cell, B cell native, macrophage M0 and M2, neutrophil and T cell CD8 in bladder cancer. Also, GAL9 displayed elevated expression in low- than high-risk specimens while higher TIM-3 and PD1LG2 expressions were found in high-risk specimens than low-risk specimens. These data indicated that this risk model might be utilized for predicting immunotherapy response of bladder cancer.

Bladder cancer represents a complex malignancy correlated to high morbidity and mortality risks. if not treated optimally. Neoadjuvant chemotherapy has been recommended prior to radical cystectomy for bladder cancer. Although the survival benefit is nearly 5-10%, some subjects cannot respond to chemotherapy [24]. Thus, identifying predictors may distinctly reduce side effects and miss the optimal time for surgery. Here, our data suggested that high-risk patients exhibited higher sensitivity to cisplatin in comparison to low-risk individuals. Inversely, subjects with low-risk were more sensitive to methotrexate than those with high-risk. Above data were indicative that this risk model might possess the potential to predict the sensitivity to cisplatin and methotrexate for bladder cancer.

Due to high abundance, lncRNAs have distinct biological functions. Our methods identified dysregulated immune-related lncRNAs as well as established the optimal immune-related lncRNA pairs. Hence, pairs with high or low expressions only were tested not detecting expression levels of each lncRNA. Our risk signature possessed the superiority in clinical practice for distinguishing high- and low-risk patients. Due to the closely correlations to immune-related genes, the selected lncRNAs potentially participated in mediating immune microenvironment shape in bladder cancer. However, there are several limitations in our study. Firstly, more independent bladder cancer cohorts should be utilized for validating the identified prognostic immune-related lncRNA model. Furthermore, the functions of these lncRNAs and their interactions with immune-related genes will be confirmed based on in vitro and in vivo experiments.

Collectively, this prognostic signature constructed by 15 immune-related lncRNA pairs as an independent predictor displayed the favorable performance in predicting prognoses of bladder cancer. Also, it had the potential to predict immune landscape and chemotherapeutic response for bladder cancer patients.

Materials And Methods

Data acquirement

Transcriptome profiles of bladder cancer (n=414) and normal bladder specimens (n=19) were retrieved from TCGA project (https://tcga-data.nci.nih.gov/tcga/). Through Ensembl (http://asia.ensembl.org), the Gencode (version 26) GTF file was obtained to annotate and differentiate mRNAs and lncRNAs [25]. Following removing specimens without clinical information or those with survival time of 0 day, 408 specimens were retained and complete clinical features were listed in **Supplementary table 1**.

Identifying immune-related lncRNAs

Totally, immune-related genes were obtained from the ImmPort database (http://www.immport.org). **Supplementary table 2** listed the detailed information of these immune-related genes. Through Pearson correlation analyses, this study assessed the correlations between immune-related genes and extracted lncRNAs. The immune-related lncRNAs were screened according to correlation coefficient>0.4 and p<0.001.

Identifying dysregulated immune-related lncRNAs

Differential expression analyses of the immune-related lncRNAs between tumor and normal bladder specimens were screened utilizing limma package [26]. The lncRNAs with |log fold-change|>1.5 and false discovery rate (FDR)<0.05. Above lncRNAs were visualized by heatmap package.

Pairing dysregulated immune-related lncRNAs

Cyclically singly paring dysregulated immune-related lncRNAs were screened. The 0-or-1 matrices were developed if α = lncRNA-1 + lncRNA-2. α = 1 when lncRNA-1 expression was >lncRNA B, while α = 0 when lncRNA-1 expression was <lncRNA B. If the expression of lncRNA pair was 0 or 1, it thought there were no associations between this pair and prognoses, since the pair that did not a certain rank cannot be correctly predictive of patients' prognoses. If the number of lncRNA pairs that expression was 0 or 1 occupied >20% of entire pairs, this was an effective match.

Establishing a prognostic risk model

Prognoses analyses of dysregulated immune-related lncRNAs were carried out through univariate cox regression models. LncRNAs with p<0.05 could impact survival outcomes of bladder cancer. These lncRNAs were put into Least Absolute Shrinkage and Selector Operation (LASSO) model via glmnet package [27]. Penalty parameter tuning was carried out through ten-fold cross-verification. This analysis was run lasting 1,000 cycles. The frequency of every pairing in the 1,000-times-repeated LASSO model was retained and pairing with frequency >100 times was chosen for constructing this model. Afterwards, a multivariate Cox regression model was conducted for determining the risk score (RS) through the coefficients and expressions of candidate lncRNA pairs.

Evaluating the predictive efficacy of the prognostic risk model

Receiver operator characteristic (ROC) curves were depicted for assessing one-, three- and five-year overall survival (OS). By calculating the area under the curve (AUC), the predictive efficacy of the prognostic risk model was determined. The Akaike information criterion (AIC) value of each point for the one-year ROC curves was calculated for identifying the maximum inflection point, which was selected as the cut-off value for distinguishing patients into high and low risk subgroups. Survival status of each subgroup was visualized. Prognoses analyses of high and low risk subgroups were conducted through Kaplan-Meier curves. Differences in survival were determined with log-rank tests.

Clinical feature assessment of the risk model

Associations between RS and clinical features (survival status, age, gender, grade, stage, T, N and M) were evaluated with chi-square tests. Also, RS was compared among different subgroups according to these clinical features. Univariate cox regression analyses were conducted for screening which factors could impact patients' survival. Hazard ratio and p values were separately calculated. Utilizing multivariate cox regression analyses, indicators that were independently predictive of survival were determined. One-year ROC curves were plotted for comparing the predictive performance of risk model and other clinical features.

Analysis of immune cell infiltrations

The known algorithms that included TIMER (version 2.0; http://timer.cistrome.org/) [28], CIBERSORT (http://cibersort.stanford.edu/) [29], XCELL (http://xCell.ucsf.edu/) [30], QUANTISEQ (http://icbi.at/quantiseq) [31], Microenvironment Cell Populations-counter (MCPcounter) [32] and EPIC (http://epic.gfellerlab.org) [33] were employed for inferring immune cell infiltrations of bladder cancer specimens on the basis of gene expression profiling. Spearman correlation analyses were carried out for estimating the associations between RS and immune cell infiltrations. Immune cell infiltrations between high- and low-risk subgroups were compared through Wilcoxon tests. Immune cells with $p<0.05$ were screened and visualized into a lollipop diagram utilizing ggplot2 package.

Associations between immune checkpoints and risk model

The expression of immune checkpoints (CTLA4, LAG3, PDL1, PD1, TIGIT, GAL9, TIM-3 and PD1LG2) was quantified in every bladder cancer specimen. Their expressions were compared between high- and low-risk subgroups.

Estimating the associations between chemosensitivity and risk model

The half inhibitory concentration (IC50) of chemotherapy drugs (cisplatin, methotrexate, vinblastine, gemcitabine and doxorubicin) was determined in every bladder cancer specimen utilizing pRRophetic package [34]. The differences in IC50 were compared between high- and low-risk subgroups.

Statistical analyses

This study utilized R software (version 4.0.0: http://www.r-project.org) for conducting statistical analyses. The differences between two subgroups were estimated utilizing Wilcoxon rank sum tests. Meanwhile, three or more groups were compared through Kruskal-Wallis test. All statistical tests were two-sided when $p < 0.05$ indicated statistical significance.

Abbreviations

RNA-seq: RNA sequencing; TCGA: The Cancer Genome Atlas; lncRNAs: long noncoding RNAs; FDR: false discovery rate; LASSO: Least Absolute Shrinkage and Selector Operation; RS: risk score; ROC: receiver operator characteristic; OS: overall survival; AUC: area under the curve; AIC: Akaike information criterion; MCPcounter: Microenvironment Cell Populations-counter; IC50: half inhibitory concentration.

Declarations

Data Availability:

All data generated or analyzed during this study are included in this article.

Conflicts of interest:

The authors declare that they have no competing interests.

Author contributions:

Jian Hou and Songwu Liang wrote the main manuscript text, Genyi Qu and Yong Xu performed experiments, Zhimin Xie, Guang Yang and Cheng Tang collected data, All the authors reviewed the manuscript and discussed the results and edited the manuscript.

Acknowledgments:

This work was supported in part by grants from Zhuzhou City Science and Technology Plan Project (#2019-001).

References

1. Patel, V. G., Oh, W. K. & Galsky, M. D. Treatment of muscle-invasive and advanced bladder cancer in 2020. *CA Cancer J Clin* **70**, 404-423, doi:10.3322/caac.21631 (2020).
2. Li, Y. *et al.* Non-coding RNA in bladder cancer. *Cancer Lett* **485**, 38-44, doi:10.1016/j.canlet.2020.04.023 (2020).
3. Afonso, J., Santos, L. L., Longatto-Filho, A. & Baltazar, F. Competitive glucose metabolism as a target to boost bladder cancer immunotherapy. *Nat Rev Urol* **17**, 77-106, doi:10.1038/s41585-019-0263-6 (2020).
4. Schneider, A. K., Chevalier, M. F. & Derré, L. The multifaceted immune regulation of bladder cancer. *Nat Rev Urol* **16**, 613-630, doi:10.1038/s41585-019-0226-y (2019).
5. Takeyama, Y. *et al.* Myeloid-derived suppressor cells are essential partners for immune checkpoint inhibitors in the treatment of cisplatin-resistant bladder cancer. *Cancer Lett* **479**, 89-99, doi:10.1016/j.canlet.2020.03.013 (2020).
6. Xue, Y. *et al.* Tumor-infiltrating M2 macrophages driven by specific genomic alterations are associated with prognosis in bladder cancer. *Oncol Rep* **42**, 581-594, doi:10.3892/or.2019.7196 (2019).
7. Chen, C. *et al.* Exosomal long noncoding RNA LNMAT2 promotes lymphatic metastasis in bladder cancer. *J Clin Invest* **130**, 404-421, doi:10.1172/jci130892 (2020).
8. Quan, J. *et al.* LncRNA as a diagnostic and prognostic biomarker in bladder cancer: a systematic review and meta-analysis. *OncoTargets and therapy* **11**, 6415-6424, doi:10.2147/ott.S167853 (2018).
9. Zheng, R. *et al.* Exosome-transmitted long non-coding RNA PTENP1 suppresses bladder cancer progression. *Mol Cancer* **17**, 143, doi:10.1186/s12943-018-0880-3 (2018).
10. Robertson, A. G. *et al.* Comprehensive Molecular Characterization of Muscle-Invasive Bladder Cancer. *Cell* **171**, 540-556.e525, doi:10.1016/j.cell.2017.09.007 (2017).

11. Tran, L., Xiao, J. F., Agarwal, N., Duex, J. E. & Theodorescu, D. Advances in bladder cancer biology and therapy. *Nat Rev Cancer* **21**, 104-121, doi:10.1038/s41568-020-00313-1 (2021).
12. Yu, Y. *et al.* Association of Long Noncoding RNA Biomarkers With Clinical Immune Subtype and Prediction of Immunotherapy Response in Patients With Cancer. *JAMA Netw Open* **3**, e202149, doi:10.1001/jamanetworkopen.2020.2149 (2020).
13. Ho, K. H. *et al.* Glycolysis-associated lncRNAs identify a subgroup of cancer patients with poor prognoses and a high-infiltration immune microenvironment. *BMC Med* **19**, 59, doi:10.1186/s12916-021-01925-6 (2021).
14. Cao, R., Yuan, L., Ma, B., Wang, G. & Tian, Y. Immune-related long non-coding RNA signature identified prognosis and immunotherapeutic efficiency in bladder cancer (BLCA). *Cancer Cell Int* **20**, 276, doi:10.1186/s12935-020-01362-0 (2020).
15. Wang, J. *et al.* Identification and verification of an immune-related lncRNA signature for predicting the prognosis of patients with bladder cancer. *Int Immunopharmacol* **90**, 107146, doi:10.1016/j.intimp.2020.107146 (2021).
16. Wu, Y. *et al.* Identification of immune-related LncRNA for predicting prognosis and immunotherapeutic response in bladder cancer. *Aging (Albany NY)* **12**, 23306-23325, doi:10.18632/aging.104115 (2020).
17. Zhou, M. *et al.* Computational recognition of lncRNA signature of tumor-infiltrating B lymphocytes with potential implications in prognosis and immunotherapy of bladder cancer. *Brief Bioinform* **22**, doi:10.1093/bib/bbaa047 (2021).
18. Jiang, W., Zhu, D., Wang, C. & Zhu, Y. An immune relevant signature for predicting prognoses and immunotherapeutic responses in patients with muscle-invasive bladder cancer (MIBC). *Cancer Med* **9**, 2774-2790, doi:10.1002/cam4.2942 (2020).
19. Luo, W. J. *et al.* Construction of an immune-related LncRNA signature with prognostic significance for bladder cancer. *J Cell Mol Med* **25**, 4326-4339, doi:10.1111/jcmm.16494 (2021).
20. Hong, W. *et al.* Immune-Related lncRNA to Construct Novel Signature and Predict the Immune Landscape of Human Hepatocellular Carcinoma. *Mol Ther Nucleic Acids* **22**, 937-947, doi:10.1016/j.omtn.2020.10.002 (2020).
21. Zhang, L. *et al.* Identification of Immune-Related lncRNA Signature to Predict Prognosis and Immunotherapeutic Efficiency in Bladder Cancer. *Front Oncol* **10**, 542140, doi:10.3389/fonc.2020.542140 (2020).
22. Cao, R. *et al.* An EMT-related gene signature for the prognosis of human bladder cancer. *J Cell Mol Med* **24**, 605-617, doi:10.1111/jcmm.14767 (2020).
23. Wang, L. *et al.* A six-gene prognostic model predicts overall survival in bladder cancer patients. *Cancer Cell Int* **19**, 229, doi:10.1186/s12935-019-0950-7 (2019).
24. Motterle, G., Andrews, J. R., Morlacco, A. & Karnes, R. J. Predicting Response to Neoadjuvant Chemotherapy in Bladder Cancer. *Eur Urol Focus* **6**, 642-649, doi:10.1016/j.euf.2019.10.016 (2020).
25. Yates, A. D. *et al.* Ensembl 2020. *Nucleic Acids Res* **48**, D682-d688, doi:10.1093/nar/gkz966 (2020).

26. Ritchie, M. E. *et al.* limma powers differential expression analyses for RNA-sequencing and microarray studies. *Nucleic acids research* **43**, e47, doi:10.1093/nar/gkv007 (2015).
27. Friedman, J., Hastie, T. & Tibshirani, R. Regularization Paths for Generalized Linear Models via Coordinate Descent. *Journal of statistical software* **33**, 1-22 (2010).
28. Li, T. *et al.* TIMER2.0 for analysis of tumor-infiltrating immune cells. *Nucleic Acids Res* **48**, W509-w514, doi:10.1093/nar/gkaa407 (2020).
29. Newman, A. M. *et al.* Robust enumeration of cell subsets from tissue expression profiles. *Nat Methods* **12**, 453-457, doi:10.1038/nmeth.3337 (2015).
30. Aran, D., Hu, Z. & Butte, A. J. xCell: digitally portraying the tissue cellular heterogeneity landscape. *Genome Biol* **18**, 220, doi:10.1186/s13059-017-1349-1 (2017).
31. Finotello, F. *et al.* Molecular and pharmacological modulators of the tumor immune contexture revealed by deconvolution of RNA-seq data. *Genome Med* **11**, 34, doi:10.1186/s13073-019-0638-6 (2019).
32. Becht, E. *et al.* Estimating the population abundance of tissue-infiltrating immune and stromal cell populations using gene expression. *Genome Biol* **17**, 218, doi:10.1186/s13059-016-1070-5 (2016).
33. Racle, J. & Gfeller, D. EPIC: A Tool to Estimate the Proportions of Different Cell Types from Bulk Gene Expression Data. *Methods Mol Biol* **2120**, 233-248, doi:10.1007/978-1-0716-0327-7_17 (2020).
34. Geeleher, P., Cox, N. & Huang, R. S. pRRophetic: an R package for prediction of clinical chemotherapeutic response from tumor gene expression levels. *PLoS One* **9**, e107468, doi:10.1371/journal.pone.0107468 (2014).

Figures

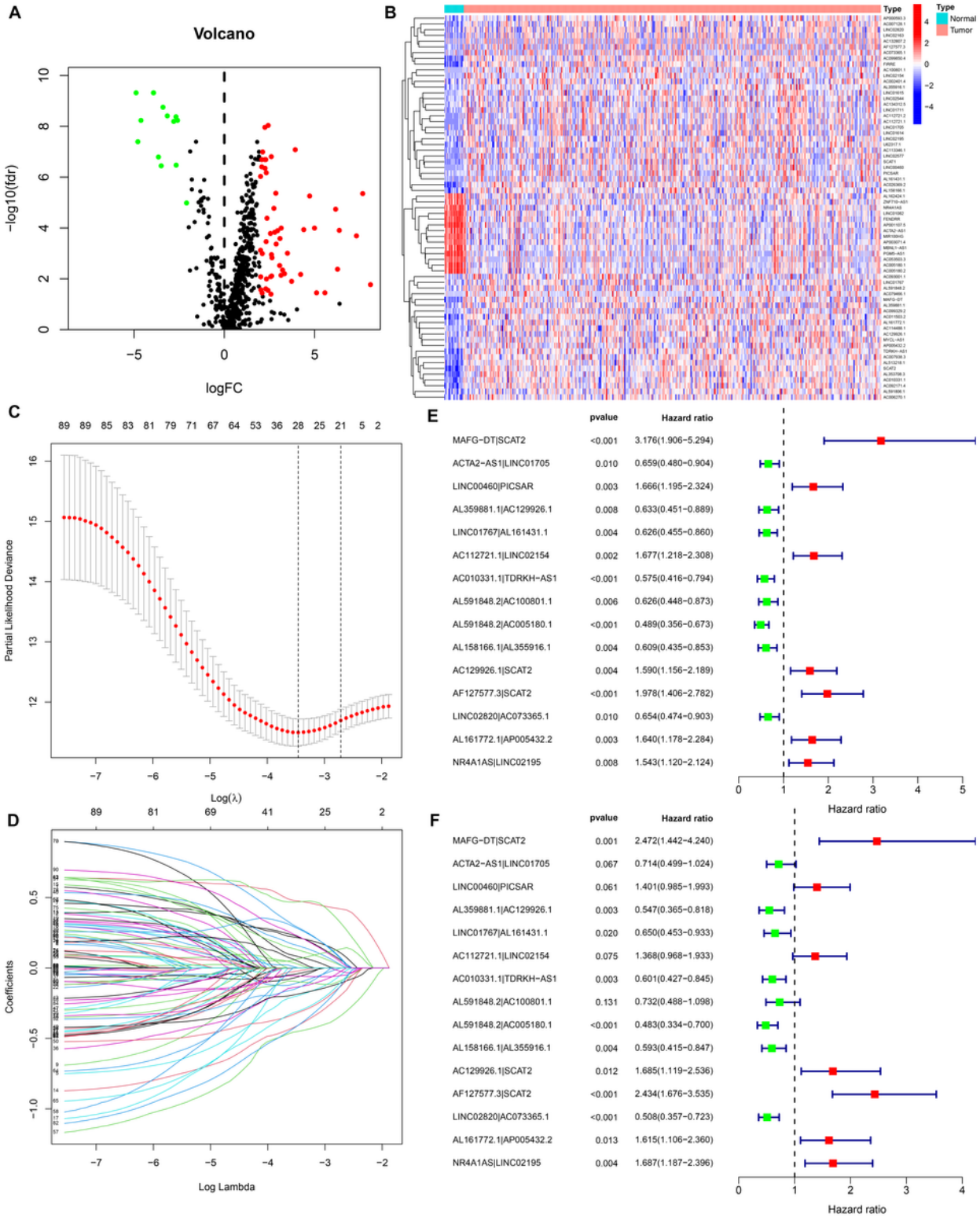

Figure 1

Developing a prognostic immune-related lncRNA signature for bladder cancer. (A) Volcano diagram of immune-related lncRNAs that displayed abnormal expression in bladder cancer and normal tissue specimens. Red dots: up-regulation and green dots: down-regulation. (B) Hierarchical clustering analyses of the dysregulated expression patterns of these immune-related lncRNAs between bladder cancer and normal tissue specimens. Red: up-regulation and blue: down-regulation. (C) Elucidating LASSO coefficient

profiling of these prognostic lncRNAs. (D) Validating tuning parameter selection for LASSO regression model. (E) Univariate cox regression analyses of the dysregulated immune-related lncRNAs that may significantly impact bladder cancer's survival. Red: risk factor and green: protective factor. (F) Multivariate Cox regression analyses of the candidate prognostic lncRNAs.

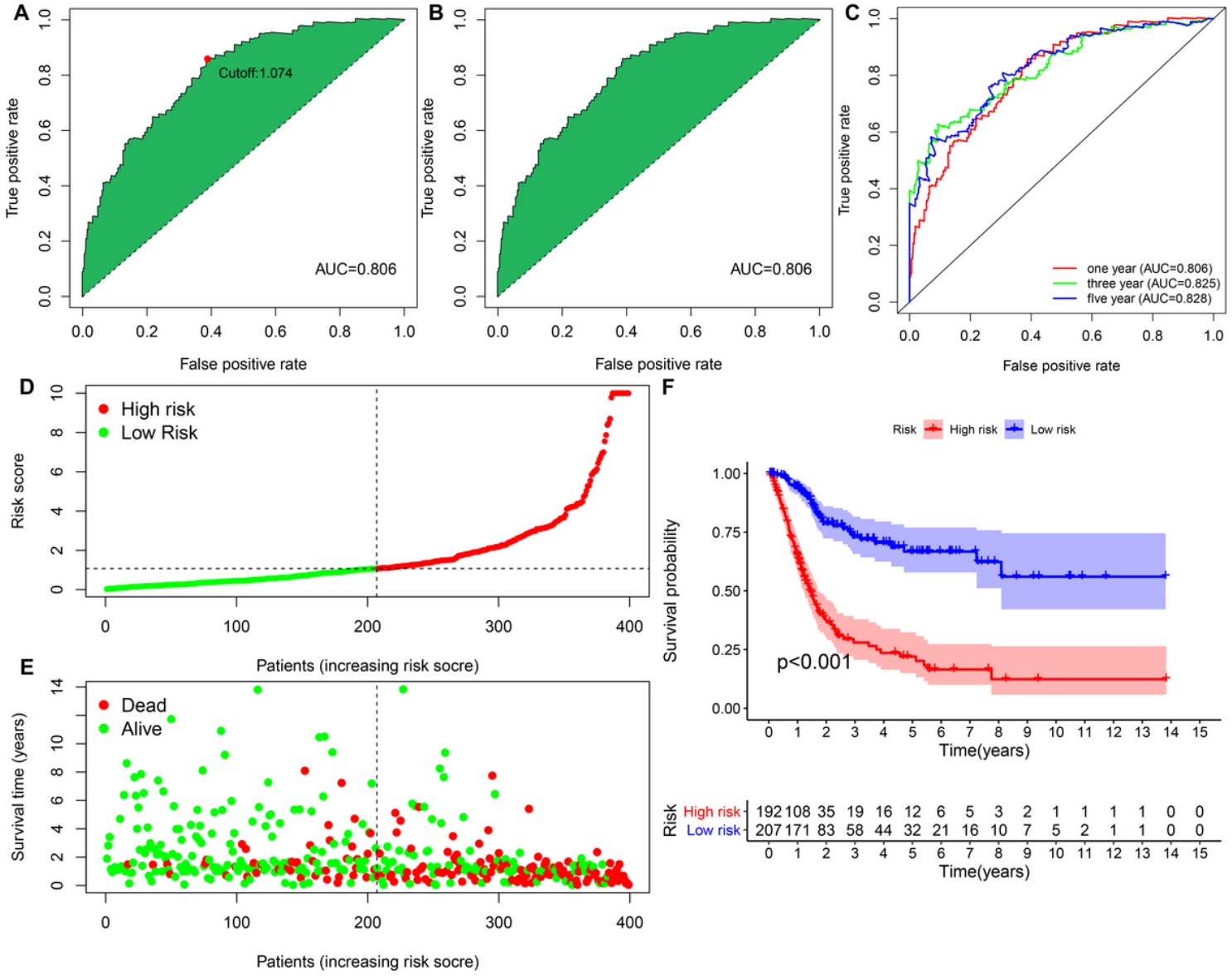

Figure 2

Evaluating the predictive performance of this immune-related lncRNA signature on bladder cancer prognoses. (A) ROC curves of the immune-related lncRNA signature for bladder cancer subjects. The maximum inflection point was the cut-off point that was calculated with the AIC method. (B) Calculating the AUC value for evaluating the predictive efficacy of this signature in bladder cancer prognoses. (C) The one-, three- and five-year ROC curves of this signature. (D) Calculating the risk score of each bladder cancer subject and distinguishing patients into high and low risk subgroups based on the cutoff value (vertical dotted line). Red: high risk and green: low risk. (E) Visualizing the distribution of survival status in high and low risk bladder cancer subjects. Red dots: alive and green dots: alive. Vertical dotted line

represented the cutoff value of two subgroups. (F) Kaplan-Meier curves of overall survival between high and low risk patients.

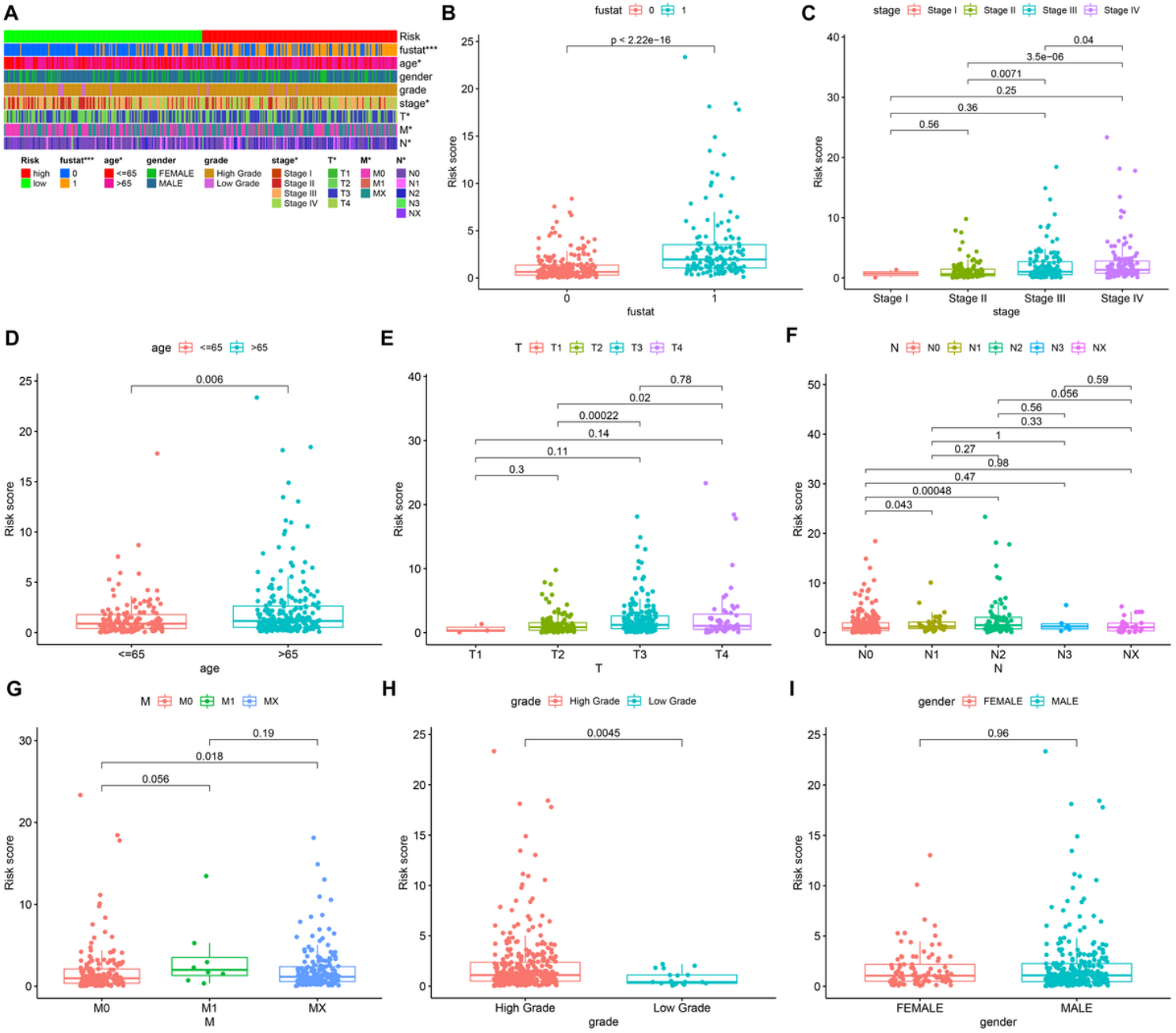

Figure 3

Associations between this prognostic immune-related lncRNA signature and clinicopathological characteristics of bladder cancer. (A) Heatmaps of the visualization of clinicopathological characteristics: survival status, age, gender, grade, stage, T, N and M in high and low bladder cancer subjects. *p<0.05; ***p<0.001. Comparing the risk score in different clinicopathological characteristics: (B) survival status (0: dead; 1: alive), (C) stage I-IV, (D) age ≤65 and >65, (E) T1-4, (F) N0-X, (G) M0-X, (H) grade and (I) gender.

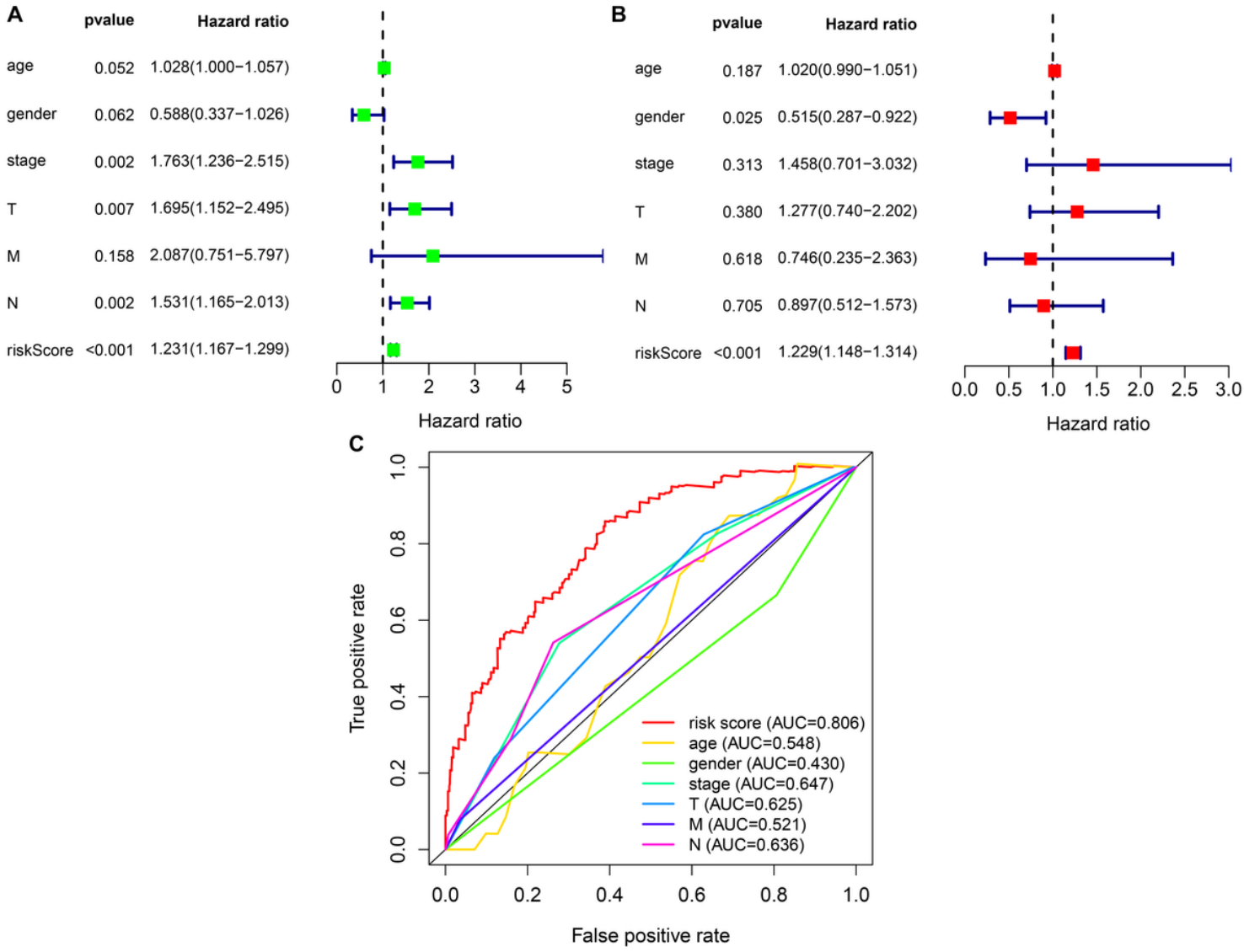

Figure 4

Assessing the predictive independency of this prognostic immune-related lncRNA signature for bladder cancer prognoses. (A) Univariate cox regression analyses of the correlations of age, gender, stage, T, N, M and risk score with bladder cancer prognoses. (B) Multivariate cox regression for evaluating the independent predictive factors. (C) Comparing the AUC values of age, gender, stage, T, N, M and risk score.

Figure 5

Correlations between risk score and immune cell infiltrations of bladder cancer specimens by following software: XCELL; TIMER; QUANTISEQ; MCPCOUNTER; EPIC; CIBERSORT-ABS and CIBERSORT.

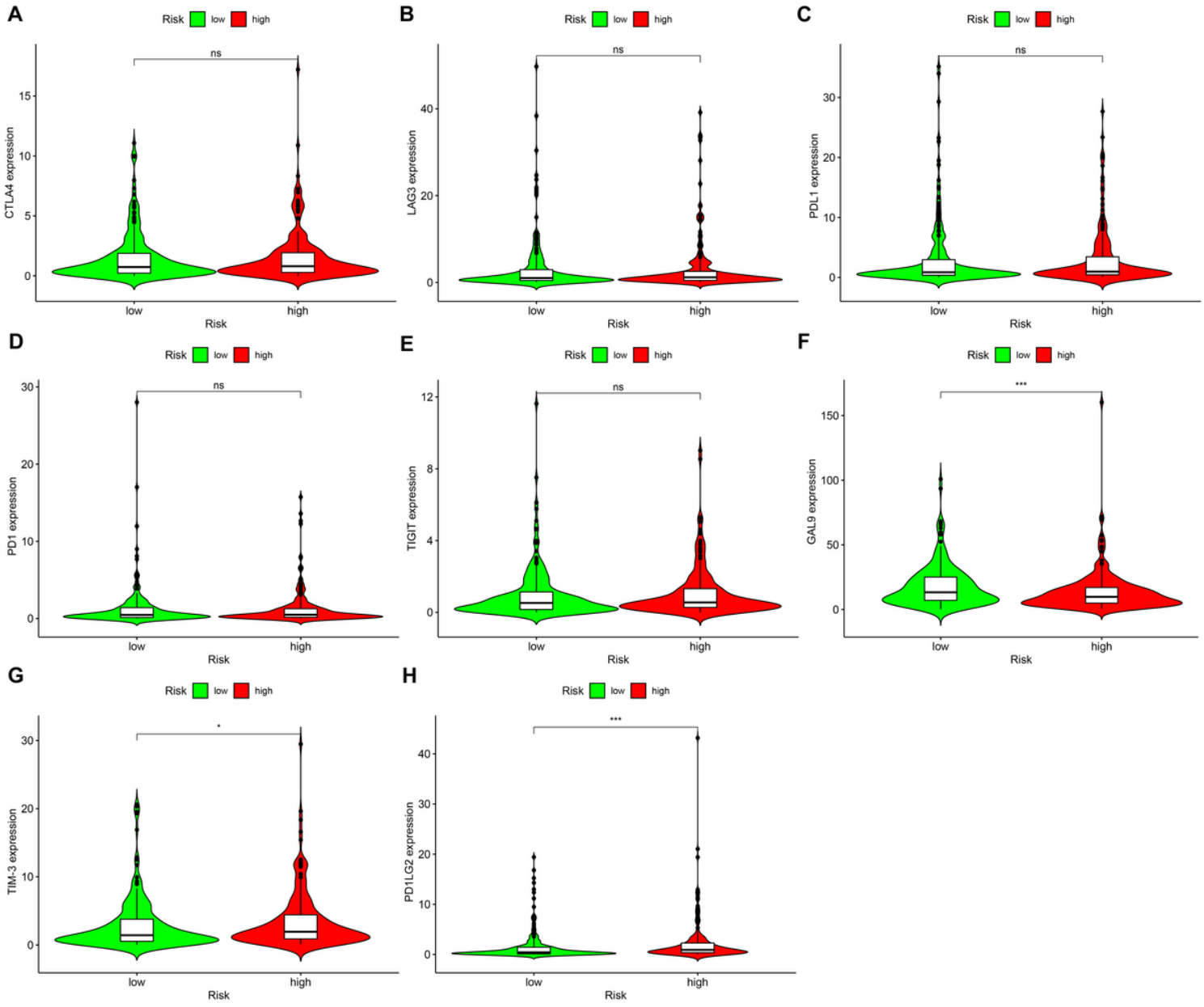

Figure 6

Correlations between risk model and immune checkpoints in bladder cancer. Comparing the expressions of (A) CTLA4; (B) LAG3; (C) PDL1; (D) PD1; (E) TIGIT; (F) GAL9; (G) TIM-3 and (H) PD1LG2 in high and low bladder cancer subjects. Ns: not significant; *p<0.05; ***p<0.001.

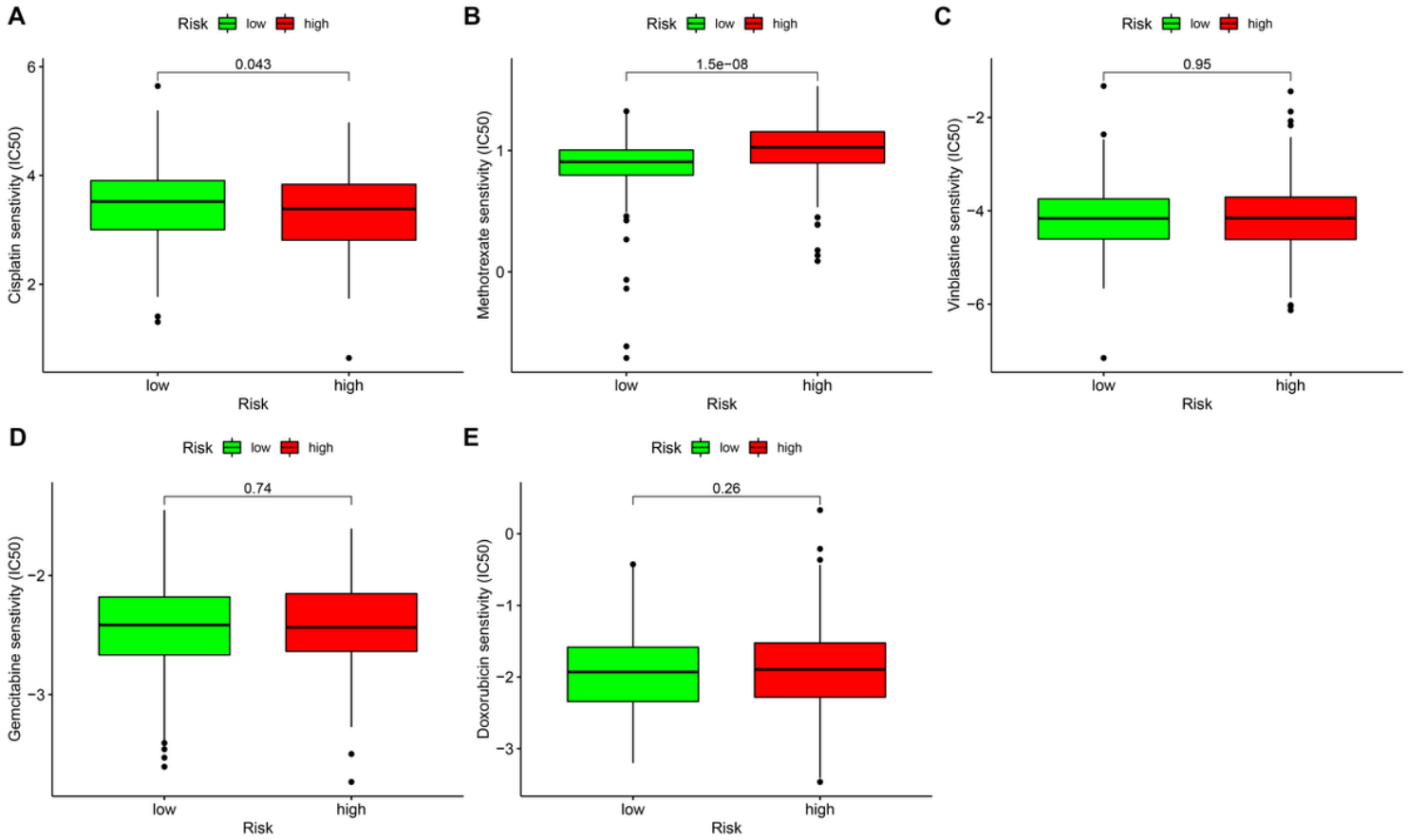

Figure 7

Correlations between risk model and the sensitivity to chemotherapy drugs in bladder cancer. Comparing the IC50 values of (A) cisplatin; (B) methotrexate; (C) vinblastine; (D) gemcitabine and (E) doxorubicin in high and low bladder cancer subjects.

Supplementary Files

This is a list of supplementary files associated with this preprint. Click to download.

- Supplementaryfigure1.tif
- Supplementarytable1.xlsx
- Supplementarytable2.xlsx
- Supplementarytable3.xlsx
- Supplementarytable4.xlsx